Comparative Experiment with DFT and TD-DFT Study of Berry Dye Chelated TiO$_2$ for Dye-Sensitized Solar Cell (DSSC)

Muthaiyan L[1], Sriram S[2], Jeyaprakash BG[1,2], Balamurugan D[1,2*]

[1]*Functional Nanomaterials Lab, Centre for Nanotechnology & Advanced Biomaterials (CeNTAB), School of Electrical & Electronics Engineering, SASTRA University, Thanjavur-613401, Tamil Nadu, India*
[2]*Department of Physics, School of Electrical & Electronics Engineering, SASTRA University, Thanjavur-613401, Tamil Nadu, India*

ABSTRACT

Combined experimental and theoretical approach empathize the importance of anchoring group (hydroxyl group) properties present in berry dye (pelargonidin). Titanium Dioxide (TiO$_2$) nanostructure has a tendency of electron transfer property from dye to TiO$_2$ photoanode. X-rey Diffraction (XRD) and Field Emission Scanning Electron Microscope (FESEM) studies show the formation of TiO$_2$ spherical shaped nanocrystallite. The berry dye and dye-sensitized TiO$_2$ thin film were investigated by UV-Visible spectra and Fourier Transform Infrared (FTIR) spectra results were compared experimental and theoretical data. Density Functional Theory (DFT) is adopted for study anthocyanidin compound: pelargonidin dye present in the natural berry shows good oscillator strength (f) and Light Harvesting Efficiency (LHE). Hence, pelargonidin/TiO$_2$ system also has significant responses in the Density of State (DOS) and Frontier Molecular Orbital (FMO).

Keywords: DSSC, Pelargonidin, LHE, DOS

INTRODUCTION

Dye Sensitized Solar Cells (DSSC) has significant attention in scientific world, due to low cost, semi-flexible, semi-transparent, and highly efficient and environment friendly compared to silicon solar cell, developed by O'Regan and Grätzel in 1991 [1]. Sensitizers play a crucial role, to absorb the solar energy and to convert into electric charge. Two different types of dye molecules: metal-free organic and metal organic complexes. Metal organic dyes are ruthenium-based dyes achieved the highest efficiency of 12.3% under standard illumination AM 1.5 irradiation, such as other black dye and N3/N719 dye [2]. Heavy metal ions present in metal based dyes are not environmental friendly and also due less availability of Ru metals have attracted the metal-free organic dyes. Instead of Ru metal complexes, metal-free organic dyes has wide advantages higher molecular excitation coefficients and low preparation cost. However, they are easy to prepare and very cheap compared to metal complexes dyes.

Recently porphyrin dyes prepared synthetically has achieved 13% efficiency [3]. Noble metal ruthenium is limited in environment and having high productivity cost, incomplete degradation lead to toxicity which considered as a main drawback. Organic dyes are best way to overcome these problems, organic dyes are natural pigments which was extracted from different part of plants such as fruit, flower, wood and stems. Organic dyes have a several advantages over synthetic dyes, such as low cost, environmental friendly, availability of resource. A DSSC fabricated with a wide band gap semiconductor such as TiO$_2$, ZnO, SnO$_2$ semiconductor sensitized with molecular dyes, electrolyte containing Iodide/triiodide (I$^-$/I$_3^-$) redox couple and platinum counter electrode.

The photon absorption and transportation of electron is carried out from sensitized dye to metal oxide semiconductor. The ideal sensitizer should have property to absorb light below a threshold wavelength 920 nm [4]. Feng et al. [5] has reported metal-free donor-π-bridge molecule has property to transfer maximum amount of electrons are injected to the conduction band of semiconductor TiO$_2$ suggested that ullazine donor-π-bridge group can be an excellent dye sensitizer for future DSSC applications. Therefore, extensive studies on different metal-free organic dye molecules are coumarin, triarylamine, hemocyanin, perylene, phthalocyanine, indoline, anthocyanidins and anthocyanin studies indicate that, these dye efficiencies are less, due to weak binding energy with metal oxide semiconductors and less absorption in the visible region.

Mohr et al. [6] have reported anthocyanin dye sensitizers using the hybrid method to find the properties and dynamics of dyes using (DFT) and Time Dependent-Density Functional Theory (TD-DFT). The result showed the anthocyanin has the potential to absorb the near UV region and studied the photon induced electron from the dye to TiO$_2$. The flavylium compound present in berry consists of anthocyanin pigments and anthocyanidin pigments [7]. Anthocyanidins pigments colour ranges from salmon pink through red, violet to dark blue present in fruits, leaves, stems, roots, berry and flowers.

Dye consists of two aromatic rings (A and C) are base rings, connected to a third ring (B) [8]. Anthocyanidin pigments with substituted –OH in B ring are known as pelargonidin shown in Figure 1. Pelargonidin are rich in blueberry, blackberry, strawberry, cranberry and bilberry [9,10]. In this work, comparative study of experimental characterization of berry dye-sensitized TiO_2 thin film with pelargonidin/TiO_2 system were investigated using computational methods to understand the electronic properties and to increase the performance of electron transfer mechanism in DSSC.
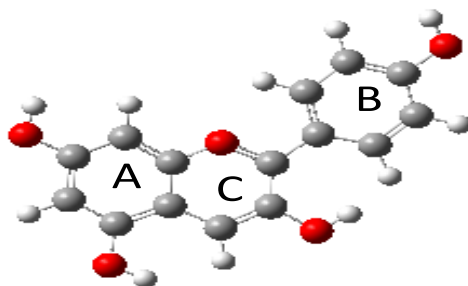

Figure 1: The structure of pelargonidin dye

MATERIALS AND METHODS

Preparation of TiO_2 photoanode thin film

0.2 g of TiO_2 powder (98% pure) is taken in a mortar and continuously pulverised for 15 min. Add 0.2 g of Poly Ethylene Glycol (PEG-4000) and mixed with TiO_2 in a mortar and grinded for 10 min and finally, 1.5 ml of terpineol added and mixed together until titanium dioxide paste is uniform. The active area is determined by taping four sides on Indium Tin Oxide (ITO) substrate by doctor blade method. TiO_2 paste is uniformly distributed on the active area of ITO substrate by doctor blade method and coated TiO_2 thin film is left at room temperature for few minutes. Tapes are removed and the then coated film is annealed for 30 min at 350°C. TiO_2 thin film left in a furnace to slowly cool down to room temperature [11].

Dye preparation

10 g of berry is mixed with 10 ml of ethanol with a ratio of 1:1 and meshed to form a juicy solution and then extracted 20 ml berry juice is kept inside the ultrasonic cleaner for 15 min at 30°C temperature with the frequency of 20 Hz for dispersion. Centrifuge (5000 rpm for 30 min) is carried out to filter the pure berry solution.

Berry sensitised electrode

TiO_2 thin film is sensitised in the extracted berry dye solution for 24 h in a petri dish and then covered with aluminium foil at room temperature kept in dark room.

Computational methods

DFT were used for calculating the geometrical structural analysis of pelargonidin dye in the ground states and excited states were studied using the TD-DFT. Hybrid functional Becke's three parameters and Lee-Yang-Parr (B3LYP) with 6-31G(d,p) basis sets was used for optimising the dyes were performed using Gaussian software 09 [12,13]. The vertical excitation, maximum absorption and oscillator frequency were simulated using the TDSCF-DFT. The Intermolecular Charge Transfer (ICT) is analysed using energy level pattern of Highest Occupied Molecular Orbital (HOMO) and Lowest Unoccupied Molecular Orbital (LUMO) [14]. The Density of States (DOS) of dye adsorption on TiO_2 surface is analysed using the GaussSum software.

RESULTS AND DISCUSSION

Structural analysis of TiO_2 thin film

 Figure 2 shows XRD pattern of the TiO_2 thin film coated on ITO glass substrate, the experimental peak index (101), (112), (200), (105), (211), (204) in agreement with the standard 2θ, XRD pattern of JCPDS card no.21-1272 (anatase TiO_2 structure) [15]. The 2θ peaks at 25.4° and 48.01° confirm its anatase structure. The intensity of XRD peaks of the sample reflections confirms the anatase phase of TiO_2 nanoparticles formation.
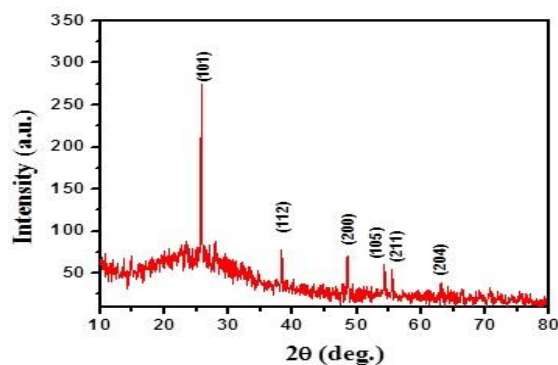

Figure 2: XRD pattern of the TiO_2 film

Surface morphology of TiO$_2$ thin film

Field Emission Scanning Electron Microscope (FESEM) image of the TiO$_2$ thin film deposited indicates a uniform spherical shaped and grain size ranges from 38.1-42 nm shown in Figure 3. Larger the surface area of TiO$_2$ nanoparticles, anchoring dye molecule will be efficiently more by providing the uniform distribution of spherical grain of nanometer size. For rapid adsorption, highly porous electrode layers with a large surface area with dyes, thus it will enhance the *Jsc* (short-circuit current density). The extensive bridging and presence of holes as an indicator of highly conducting mesoporous reveal extensive adsorption of the berry dye (pelargonidin) on the TiO$_2$ nanoparticles.
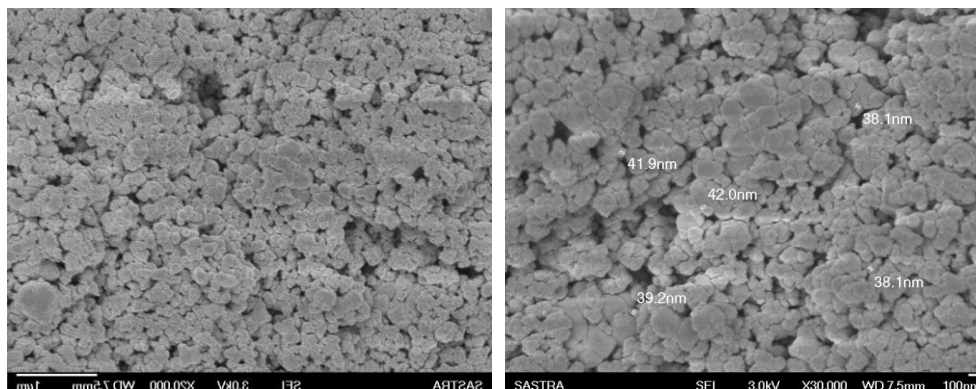

Figure 3: FESEM image of TiO$_2$ coated on ITO substrate

Optical analysis

Oprea [16] has studied the maximum absorption spectrum of the deprotonated dyes and neutral dyes, UV/Vis absorption peak of all coumarin dyes shown good results, it also matches with experimental data (NKX-2311 has maximum light harvesting property) and the electron has the tendency to localized near to the COO- group by absorbing the photons. The maximum absorbance of the berry solution is 440 nm. This decrease in transmittance, in turn, enhances the absorption of the films, thereby increasing the photon efficiency. UV-Visible absorption spectra are very intense and wide absorption band regions, dye molecule with maximum absorption wavelength at 660 nm the higher excitation is due to π→π* transition, whereas sharp peaks at 440 nm indicates n→π* transition, pelargonidin dye molecules has double excitation at near 440 nm and 528 nm are shown in Figure 4. The molar attenuation coefficient of all dyes has increased due to the presence of hydroxyl groups in B ring position of dyes. And also due to the presence of –OH (hydroxyl group) the absorption is shifted to near UV spectra with maximum extinction coefficient. The absorption bands of both graphs show that the transition to high absorption intensity and excitation energy. The efficient dye sensitizer used for DSSC should have high Light Harvesting Efficiency $_{(LHE)}$, which can be expressed by following equation [17]:

$$LHE = 1 - 10^{-f}$$
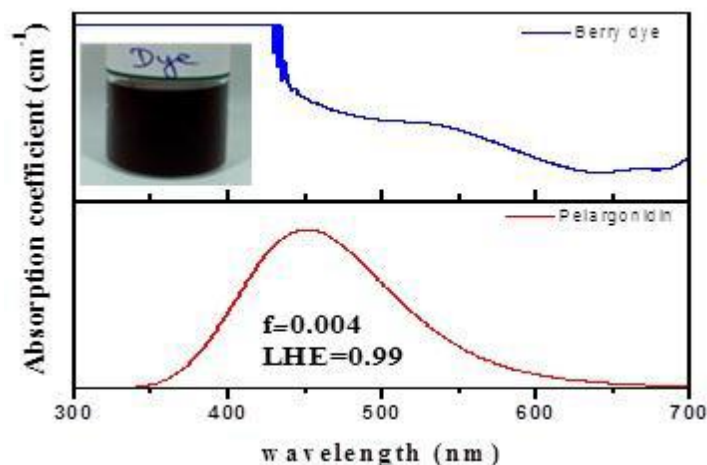
Where, f is oscillator strength.

Figure 4: UV-visible images of berry dye and pelargonidin

Functional group analysis

Fourier Transforms Infrared (FTIR) was used to characterise the functional groups present in dyes. Berry dye (pelargonidin) with the presence of –OH groups indicates that it has a tendency to anchor towards TiO$_2$ [18]. The double bond conjugation and hydroxylation are the structural property of anthocyanidins pigment that will inject electrons to the TiO$_2$ conduction band. The carbonyl and hydroxyl groups have a tendency of bonding to TiO$_2$ surface and property to transfer an electrons from the sensitizer to the TiO$_2$ conduction band. Compared experimental and theoretical results of FTIR are similar shown in Figure 5a matches in the strong O-H and C-O stretch peaks in berry dye and pelargonidin. Figure 5b also shows that strong O-H and C-C stretch peaks for berry dye-sensitized TiO$_2$ film and pelargonidin anchored to TiO$_2$.
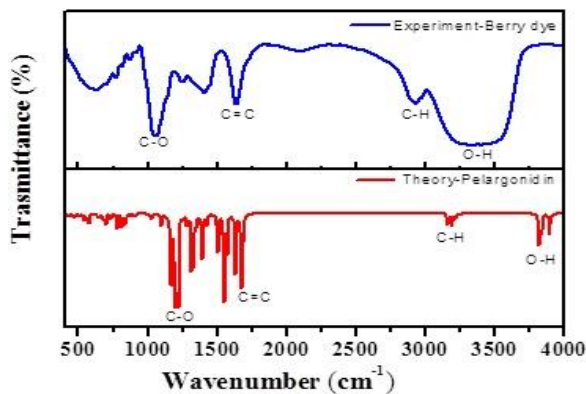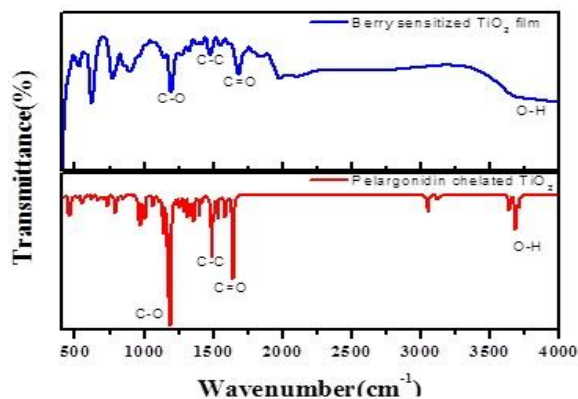
Figure 5(a): FTIR images of berry dye and pelargonidin

Figure 5(b): FTIR images of berry dye-sensitized TiO$_2$ and pelargonidin chelated TiO$_2$

Intramolecular charge transfer (ICT)

The electronic transition takes places from HOMO to LUMO (Localized for the effective charge transition at donor site). Hydroxyl group anchoring resulted in strong bonding between dye-semiconductor with oxygen atom [19]. Frontier molecular orbital energy of dye anchored to the TiO$_2$ semiconductor surface (Figure 6). In pelargonidin/TiO$_2$ system, the electron distributions in HOMOs are localised between donor group and π-spacer shown in the Figure 6c, whereas the electron distributions in LUMOs are localised between the conjugated spacer and TiO$_2$ semiconductor shown in the Figure 6d clearly indicates the intramolecular charge transferred from pelargonidin dye to TiO$_2$. DOS plot also reveals bandgap is reduced in pelargonidin/TiO$_2$ system shown in Figures 7.
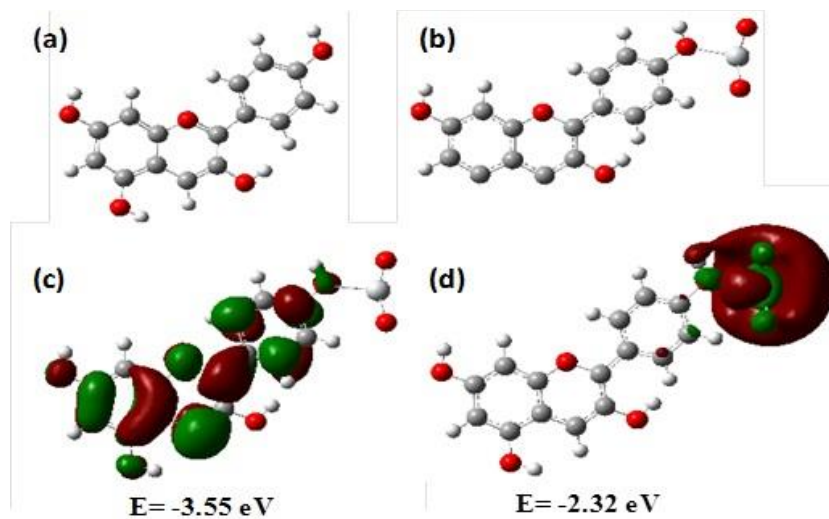
Figure 6: (a) Pelargonidin dye, (b) Pelargonidin dye chelated to TiO$_2$, (c) HOMO of pelargonidin dye chelated to TiO$_2$ and (d) LUMO of pelargonidin dye chelated to TiO$_2$
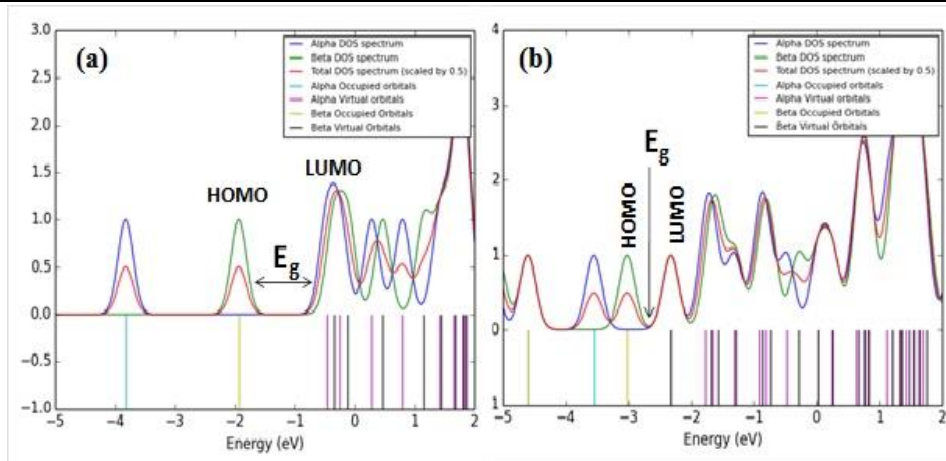
Figure 7: DOS of (a) pelargonidin dye, (b) Pelargonidin dye chelated to TiO₂

CONCLUSION

The result concludes that experimental with DFT and TD-DFT study empathise importance of anchoring group (Hydroxyl group) properties in berry dye (pelargonidin). XRD pattern confirms that the TiO_2 films contain anatase crystal structure (101) peak has high electron transport property in agreement with standard 2θ, XRD pattern of JCPDS card no.21-1272. FE-SEM image shows TiO_2 films are homogeneously distributed and spherical shaped of 38.1 nm to 42 nm nanocrystallite size. The berry dye (pelargonidin) and dye sensitised TiO_2 thin film matches with UV-Visible spectra and FTIR results of experimental and theoretical data. Pelargonidin dye present in the natural berry shown good oscillator strength (f) and LHE. Thus, the results obtained from each of the characterization studies proved that this pelargonidin/TiO_2 system has shown significant responses in generating the electrons as well as to improve efficiency. Pelargonidin dye is the potential photosensitizer for DSSC applications.

ACKNOWLEDGEMENT

REFERENCES

[1] B. O'Regan, M. Gratzel, *Nature.*, **1991**, 353, 737-739.

[2] L. Giribabu, K.R. Kumar, *Curr. Sci.,* **2013**, 104, 847-855.

[3] S. Mathew, A. Yella, P. Gao, R. Humphry-Baker, B.F.E. Curchod, N. Ashari-Astani, I. Tavernelli, U. Rothlisberger, Md. Khaja Nazeeruddin, M. Grätzel, *Nat. Chem.*, **2014**, 2, 1-6.

[4] R. Kushwaha, P. Srivastava, L. Bahadur, *J. Energy.*, **2013**.

[5] J. Feng, Y. Jiao, W. Ma, Md.K. Nazeeruddin, M. Gratzel, S. Meng, *J. Phys. Chem.*, **2012**, 117, 3772-3778.

[6] T. Mohr, V. Arulmoji, R.S. Ravindran, M. Muller, S. Ranjitha, G. Rajarajan, P.M. Anbarsan, *Spectrochim. Acta. Mol. Biomol. Spectrosc.*, **2015**, 135, 1066-1073.

[7] Iacobucci, Guillermo A, Sweeny, James G, *Tetrahedron.*, **1983**, 19, 3005-3038.

[8] F. Hernandez, P. Melgarejo, F.A. Tomas-Barberan, F. Artes, *Eur. Food. Res. Technol.*, **1999**, 210, 39-42.

[9] I. Zama, C. Martelli, G. Gorni, *Mater. Sci. Semicond. Process.*, **2017**, 61, 137-144.

[10] A. Santoni, H. Amanda, D. Darwis, *J. Chem. Pharm. Res.*, **2015**, 7, 804-808.

[11] M. Alhamed, A.S. Issa, A. Wael Doubal, *J. Electron. Devices.*, **2012**, 16.

[12] E. Piyasiri, Md.R.R. Kooh, N.T.R.N. Kumara, A. Lim, Md.I. Petra, V.N. Yoong, L.C. Ming, *Chem. Phys. Lett.*, **2013**, 585, 121-127.

[13] A.El. Assyryl, A. Hallaoui, R. Saddik, N. Benchat, B. Benali, A. Zarrouk, *Pharm. Lett.*, **2015**, 7, 295-304.

[14] Z.L. Zhang, L.Y. Zou, A.M. Ren, Y.F. Liu, J.K. Feng, C.C. Sun, *Dyes. Pigm.*, **2013**, 96, 349-363.

[15] W. Li, T. Zeng, *PLoS. One.*, **2011**, 6, 21082.

[16] C.I. Opera, P. Panait, F. Cimpoesu, M. Ferbinteanu, M.A. Girtu, *Materials.*, **2013**, 6, 2372-2392.

[17] W.R. Duncan, O.V. Prezhdo, *Annu. Rev. Phys. Chem.*, **2007**, 58, 143-84.

[18] C.R. Zhang, L. Liu, J.W. Zhe, N.Z. Jin, L.H. Yuan, Y.H. Chen, Z.Q. Wei, Y.Z. Wu, Z.J. Liu, H.S. Chen, *J. Mol. Model.*, **2013**, 19, 1553-1563.

[19] C.R. Zhang, L. Liu, J.W. Zhe, N.Z. Jin, L.H. Yuan, Y.H. Chen, Z.Q. Wei, Y.Z. Wu, Z.J. Liu, H.S. Chen, *Int. J. Mol. Sci.*, **2013**, 14, 5461-5481.